SECTION E

THE OLIVO-CEREBELLAR CIRCUIT AS A UNIVERSAL MOTOR CONTROL SYSTEM

Rodolfo R. Llinás
Department of Physiology and Neuroscience, New York University Medical School
llinar01@popmail.med.nyu.edu
Elena Leznik
Department of Physiology and Neuroscience, New York University Medical School
leznie01@popmail.med.nyu.edu
Vladimir I. Makarenko
Department of Physiology and Neuroscience, New York University Medical School
makarv02@popmail.med.nyu.edu

Abstract— Olivo-cerebellar system is one of the central networks organizing movement coordination in vertebrates. This system consists of three main anatomical structures, the inferior olive (IO), the cerebellar nuclei (CN) and the cerebellar cortex (CC). Over the last four decades studies in many laboratories have contributed significantly to our understanding of the electrophysiology of inferior olivary and cerebellar neurons. However, addressing the dynamic properties of olivo-cerebellar network requires information beyond the limits attainable using single cell recordings. Research at the neuronal network level is presently being implemented in order to determine the spatiotemporal activity profiles of ensemble neuronal activity using voltage-sensitive dye imaging. We summarize here results of such type of study using *in vitro* inferior olive slices. The dynamic characteristic of the system is addressed using the imaging results as well as mathematical modeling of the network, as a heuristic tool. A computer-based control system based on such biological findings is outlined.

***Index Terms*— Inferior Olive, oscillations, optical imaging, universal control system.**

I. Introduction

The inferior olives, the origin of the olivo-cerebellar system, project to the cerebellum via climbing fibers [1] and form one of the two major afferent pathways to the cerebellar cortex [2]. Climbing fibers innervate monosynaptically all Purkinje cells (PC) in the cerebellar cortex generating the largest synaptic junction in the vertebrate central nervous system. Indeed, activation of a climbing fiber is followed by an all or none burst of spikes [3] later known as a complex spike [4], in all of its postsynaptic PCs. On the average, an IO neuron generates ten climbing fibers [5]. In addition to contacting PCs, climbing fibers also produce collateral branches that terminate on all cerebellar nuclei [6].

IO neurons fire spontaneously at 1-10 Hz and can exhibit rhythmic oscillatory activity near 10 Hz [7], [8]. Likewise, the resulting complex spikes in the PCs are also rhythmic and have a maximum firing frequency of 10 Hz [9]. Furthermore, simultaneous electrode recordings from multiple PCs have shown that complex spikes occur synchronously in a group of PCs [10]-[12]. Such synchronous activation of multiple PCs by the IO nucleus suggests that clusters of IO neurons have the ability to fire rhythmically and in unison [13], [14]. This observation led to the proposal that climbing fibers may perform a timing function in motor coordination [15]. According to this hypothesis, IO activity functions as a motor timing signal by generating synchronous and rhythmic activation of cerebellar nuclear cells and descending and ascending connectivity to the spinal cord and thalamus. The timing control of these cerebellar nuclei on the IO is being further controlled by the synchronized inhibitory barrage originated by climbing fiber activation of PCs complex spikes. Evidence in support of this motor timing proposal includes synchronous firing of a population of PCs in anesthetized and awake animal [10], [16], [17]; recordings of rhythmic inhibitory potential in the deep cerebellar nuclei [18]; and temporal correlation between firing of the olivo-cerebellar system and the execution of movements [19].

The ability of the olivo-cerebellar system to generate synchronous rhythmic activity has been attributed to the intrinsic oscillatory properties of the IO neurons [8], [20]-[22], [23]-[25] and their electrotonic coupling [8], [13], [14], [26], [27]. In particular, several types of voltage-dependent calcium and potassium conductances, in addition to those involved in action potential generation, enable IO cells to oscillate and fire rhythmically at 1-10 Hz. These conductances include a high-threshold Ca^{2+} conductance, a somatic low-threshold Ca^{2+} conductance, a Ca^{2+}-activated K^{+} conductance, and a hyperpolarization-activated cationic conductance [8], [20], [21], [23].

Concerning the electrical coupling, as in some other CNS structures [28] gap junctions constitute the main communication pathway between the IO neurons [14], [29].

This work was supported in part by Office of Naval Research grant #N00014-02-1-0982.

Such electrotonic coupling has been proposed to play a crucial role in synchronizing IO oscillations and in generating groups of concurrently oscillating neurons [21] and has been assumed to be controlled by return glomerular inhibition [15]. IO afferents were in fact found to modulate the efficiency of electrotonic coupling via inhibition at the glomerulus where the gap junctions are located. The pathway turned out to be supported by a set of cerebellar nuclear GABAergic neurons [30] which, in addition, represent almost 50% of the total neuronal population in such nuclei, given some measure of the importance of this feedback inhibitory pathway. Indeed, it was experimentally determined that such inhibitory input can control the degree and distribution of synchronous oscillatory activity in the IO nucleus [31] and cerebellum [11], [32], [33]. Furthermore, dynamic groups of IO neurons oscillating in-phase can synchronously activate a population of PCs and thereby control patterns of synchronous activity in the cerebellum during motor coordination [19].

Although synchronized IO oscillations are a neuronal ensemble event, they have been mainly studied on a single-cell level and no information has been available about their spatial profiles. Thus, we attempted to address this issue by utilizing a voltage-sensitive dye optical imaging technique [31]. This technique is presently a methodology of choice in studying the geometrical distribution of activity in a large neuronal ensemble [34]. We have shown that ensemble oscillations in the IO emanate from ***clusters of synchronized activity***, where each cluster is a localized functional event composed of hundreds of cells. Given the distribution of complex spike activity in the cerebellar cortex, we have proposed that these clusters are very likely to be responsible for the synchronized activation of the Purkinje cells observed in previous *in vivo* multielectrode experiments [31]. Furthermore, when comparing our experimental results with those obtained by computational modeling of IO neuronal ensembles endowed with oscillatory electrical properties and electrotonic coupling [35], [36] we could show that neuronal oscillatory clustering is a direct consequence of the combined electrotonic/intrinsic properties of coupled IO neurons.

II. Optical Voltage-sensitive Imaging Results

Voltage-sensitive dye imaging of oscillatory activity was successfully implemented in rodent IO slices [31]. Following IO electrical stimuli which served to reset the phase of subthreshold oscillation and to entrain a large proportion of neurons to in-phase oscillations [21], imaging of the spatio-temporal profiles of ensemble IO oscillations were unambiguously observed. Indeed, synchronization of oscillatory activity over the IO network increased the amplitude of the optical signal to the level that could be easily detected with our imaging set-up. Such oscillatory reset was also observed with intracellular recordings from IO neurons. (Fig. 1A and 1B).

In agreement with previous intracellular results [21], an extracellular stimulation given at the dorsal border of the IO nucleus generated a full action potential followed by a membrane hyperpolarization in nearby neurons (Fig. 1A, boxed area). Our results also demonstrate that if the cell was oscillating at the time of the stimulus, its oscillations were momentarily stopped but then resumed with a different phase approximately 750 ms after the stimulation. Moreover it was also determined that such extracellular stimulation reset the phase, but not the amplitude or frequency of the subthreshold oscillation (Fig. 1B). The reset could be repeatedly observed in all cells recorded and the resulting oscillation phase shift was remarkably constant (Fig. 1B, right panel).

The optical signals

Our imaging responses consisted of an initial change in background fluorescence induced by direct electrical stimulation followed by several oscillatory waves that spread throughout the IO nucleus (Fig. 1C and 1D). These ensemble IO oscillations were calcium derived and were also observed in concurrently obtained intracellular recordings from IO neurons [31].

The optically-recorded IO oscillations consisted of clusters of coherent neuronal activity where each cluster was a localized functional entity (Fig. 1D (2^{nd} and 3^{rd} image panels). These oscillatory groupings of cells arose from several independent regions of the slice, but had the same oscillation frequency and were phase coherent. The phase coherence was most clearly observed following the phase reset triggered by the electrical stimulus. The optically-recorded oscillations were highly repeatable in time and space: the average of three oscillatory cycles had the same spatio-temporal profile as that of the individual oscillations (compare Fig. 1D 2^{nd} and 3^{rd} image panels).

Within the temporal resolution used in these experiments (4.8 ms between frames), the optical oscillations started synchronously everywhere in the slice (see Fig. 1C pixel 1, 2, 3 and 4). In our experiments, the frequency of optically-recorded clusters varied from 1.6 to 6.5 Hz which was in range for intracellularly recorded subthreshold oscillations [21], [22], [37].

The optically recorded oscillatory clusters had a dynamic spatial organization. They changed their size depending on the oscillation phase such that they embraced the largest area during the upward phase of the oscillations (Figure 1D, 2^{nd} image panel, 3^{rd} image). Hence, each cluster consisted of a core region and the adjoining area. The core region demonstrated a close to constant size, but the extent of the adjoining area was found to be phase-dependent. We calculated the core area and maximum area (i.e. the core region plus the adjoining area at its utmost extent) for several representative clusters in each experiment. The mean core area and the mean maximum area of a cluster occupied an area of several hundredth mm^2 [31].

Since most of the IO neurons are coupled via dendro-dendritic gap junctions, which are not located within the same plane [38], [39], we assumed that the optically-recorded IO

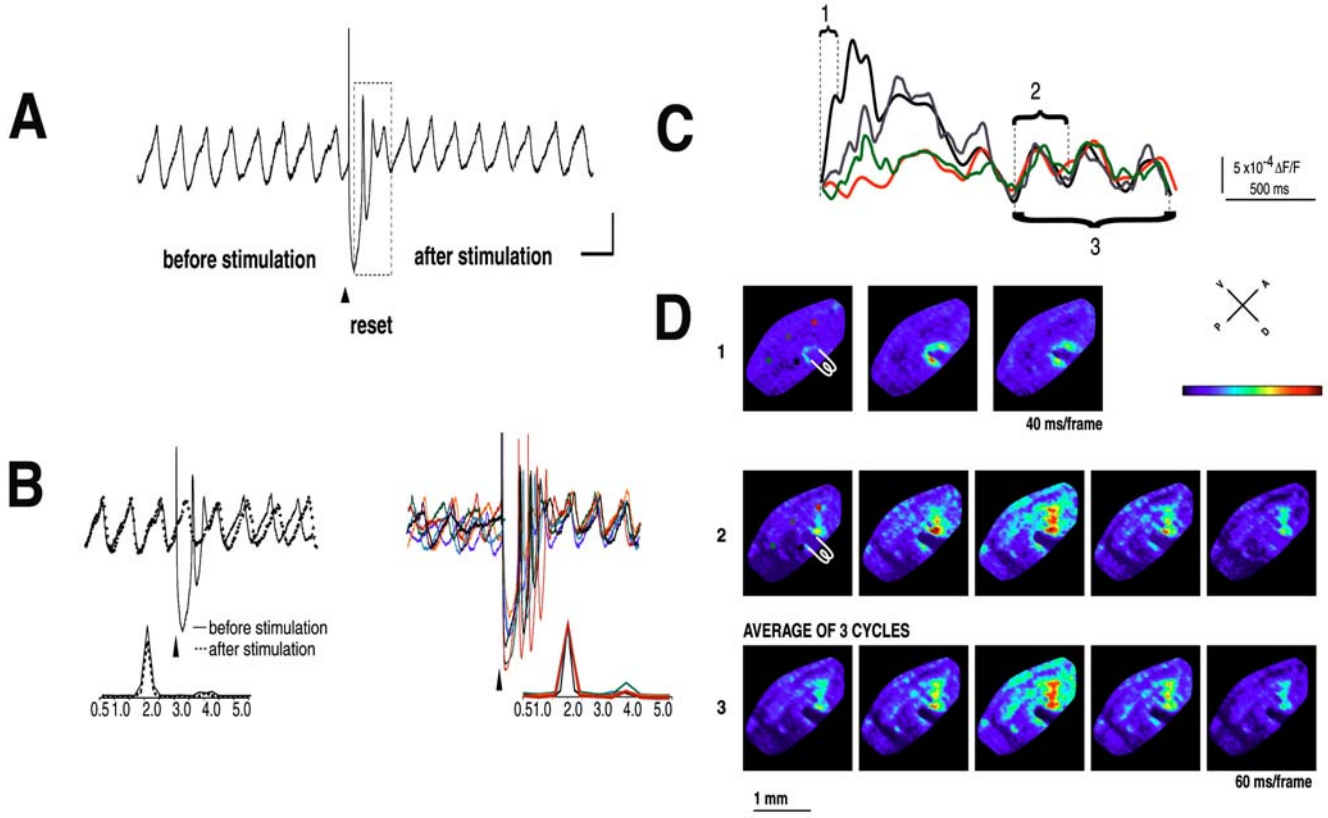

Fig. 1 **(A)** Intracellular recording of spontaneous oscillations at 2 Hz interrupted by an extracellular stimulus. After extracellular stimulation (marked with an arrow head), the oscillations disappeared for 750 ms (boxed area) and then resumed. The membrane potential was at -60 mV. **(B)** On the left, intracellular recordings of spontaneous (dashed black line) and stimulus-evoked (solid black line) oscillations from the same cell are superimposed. Their corresponding power spectra are shown below. Note that extracellular stimulation only modified the phase of spontaneous oscillations without affecting its amplitude and frequency. On the right, six individual intracellular traces of stimulus-evoked oscillations from the same cell are superimposed. Each trace is shown in a different color. Their corresponding power spectra are displayed below. In every recording, the frequency of stimulation-evoked oscillation was the same (2.0 Hz). Note that in each trace the stimulation-induced shift in the oscillatory cellular rhythm is remarkably similar. Oscillations are clearly seen after the stimulus-induced reset, but can be barely detected before the stimulation. Calibration bar: 1 mV; A, 1 sec; B, C, 500ms.**(C)** A complete time-course of optical responses for four pixels. Locations of the pixels are marked with circles of different color in D. The optical response consisted of an initial response to a train of extracellular stimuli (two stimuli at 10Hz) followed by three oscillatory cycles. The frequency of the optically recorded oscillations was 4 Hz. **(D)** Several multi-frame displays for each of the regions marked in C. Only the area of the IO is shown. Position of the stimulating electrode is indicated. The color bar gives the color scale with dark purple corresponding to lowest fluorescence and red corresponding to highest fluorescence. (1) The response of the IO nucleus to the first stimulus. (2) The location and spatial spread of one cycle of the ensemble oscillations. The oscillations emanate from several clusters of closely spaced cells throughout the IO (see the change in amplitude with time). These clusters are highly repeatable from cycle-to-cycle over the oscillation sequence. (3) An average of four oscillatory cycles further underlines the stability of fluorescent clusters. Adapted from [31].

clusters were three-dimensional structures. We measured the area of each cluster and then estimated their volume by multiplying the area of the cluster by the thickness of the live tissue in the slice. (This could be done because fluorescence can be detected up to 700 μm in depth [40] and our slices were only 300 μm thick). Next, we approximated the number of cells in each cluster by multiplying the density of the IO cells in rat (80,000 cells/mm^3) [41] by the volume of each cluster. Based on the above assumptions, we found that both the core area and the maximum area of a cluster comprised hundreds of cells.

Thus, our optical data indicate that at the network level, the IO nucleus is organized in functionally coupled activity clusters. Each cluster is comprised of several hundreds of cells, which may act in unison to simultaneously activate groups of cerebellar Purkinje cells as has been previously observed with multiple electrode recordings [10], [12], [16], [42]

Modulation of cluster dimensions

We considered the possibility that the level of functional coupling among the IO neurons defined dimensions of the optically recorded fluorescent clusters [43]. If this were the case, drugs that modulate electrical coupling among olivary neurons such as picrotoxin [11] should change cluster dimensions. Indeed, application of picrotoxin increased the size of the oscillatory clusters by partly merging them into larger areas of coherent activity and by partly activating additional neuronal regions (Fig. 2A and 2B).

These results also demonstrate that clustering was not an artifact resulting from sparse distribution of neuronal survival,

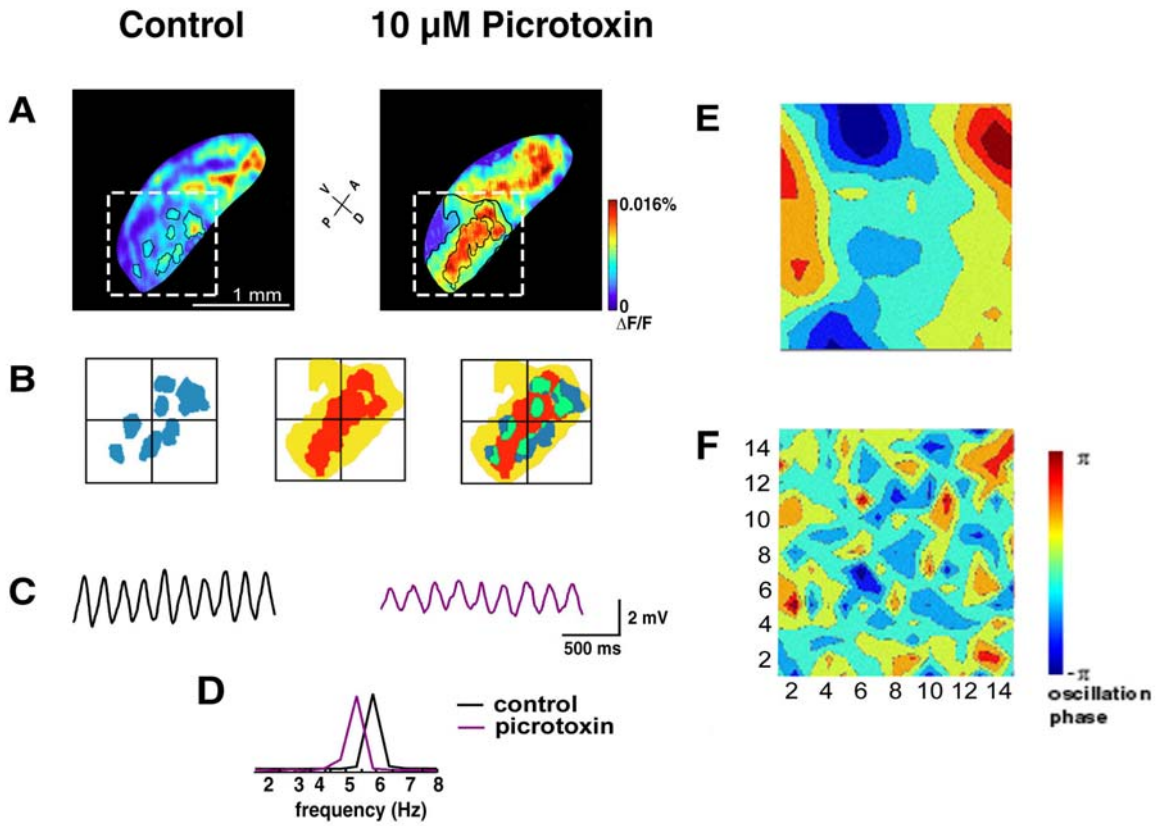

Fig. 2. **(A)** Frames of imaged ensemble neuronal oscillating clusters in control conditions (left) and after addition of 10μm of picrotoxin (right) are shown. Several representative clusters in the lower right part of the IO are outlined in black. The clusters were defined are as areas with pixel values above the selected threshold level. After picrotoxin, an additional threshold level of higher value was chosen to delineate the highest areas of activity. **(B)** Cluster's contours shown within the boxed area (1mm x 1mm) are enlarged for control condition (right panel) and after addition of picrotoxin (middle panel). On the left, areas shown in the right and middle panels are superimposed. Control clusters are shown in blue; picrotoxin clusters of lower threshold are shown in yellow and those of higher threshold are shaded in red. Overlapping regions of control clusters and picrotoxin clusters of lower threshold are shown in green. Note that picrotoxin significantly increased the size of clusters by activating addition regions and merging several small areas into larger activation areas. **(C)** Intracellular recording from an IO neuron showing spontaneous subthreshold oscillations before (in black) and after addition of 10μM picrotoxin (in blue). **(D)** Power spectra of control (blue line) and picrotoxin-modulated oscillations (blue line) are superimposed. Addition of picrotoxin reduced amplitude and frequency of subthreshold oscillations without changing the resting membrane potential of the cell. **(E and F)** Clustering in the modeled network as a function of coupling degree. **(E)** In the absence of inhibition large clusters are observed and demonstrate large fluctuations in size (as in case with picrotoxin). **(F)** In the presence of inhibition (reduced coupling) many small clusters are formed, but there is much less fluctuation in size (as in control conditions). Adapted from [31].

as neurons previously occupying quiescent sites became active following drug administration.

At the single cell level, addition of picrotoxin decreased the frequency and amplitude of spontaneous subthreshold oscillations without affecting membrane potential (Fig. 2C and 2D) which was consistent with an increased cluster size. Indeed, picrotoxin decoupled IO neurons by blocking GABAergic synapses and thus producing a shunt at the glomerulus that reduced the effective coupling among IO cells. Modulation of the effective electrotonic coupling changed cluster dimensions; and so the modulation of afferent GABAergic inputs on the IO glomeruli [29], [38] should produce the observed results. Expansion of cluster size increases the electrical load of the network resulting in a reduction of amplitude and frequency of subthreshold oscillations and an increase in a cluster size.

In conclusion, dimensions of clusters are probably determined by the IO electrical coupling coefficient, and thus, by the magnitude and distribution of the return inhibition from the cerebellar nuclear feedback as has been demonstrated in previous *in vivo* experiments [11], [44] and supported with mathematical modeling [31], [36].

III. Modeling IO Cluster Activity

As indicated above, the IO nucleus appears to play a significant role in the timing of organized movement. The anatomical and physiological properties of these neurons are sufficiently well established to warrant the development of quantitative computer modeling of both single cell and of network properties.

Present knowledge indicates that the subthreshold membrane potential oscillations of IO neurons have an important functional role and complex dynamics. The latter implies that in addition to the individual IO neuron dynamics, the electrotonic communication matrix weaved by the

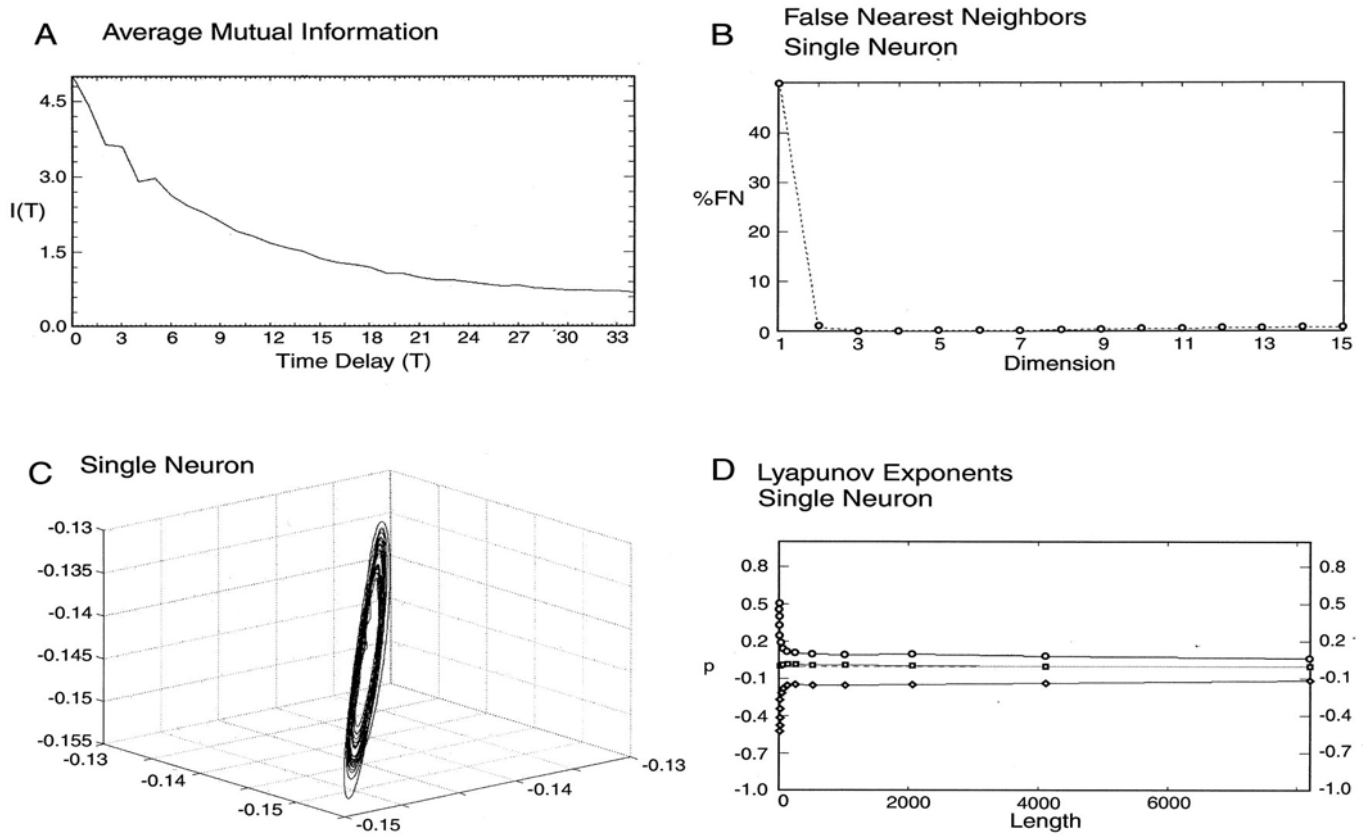

Fig. 3. Reconstruction of attractor properties from a time series analysis of membrane potential oscillation in an intracellularly recorded IO neuron in vitro. The attractor has a structure close to a limit cycle with a regular periodic trajectory. Average Mutual Information **(A)** and False Nearest Neighbors **(B)** methods were used to reconstruct the attractor **(C)** and Lyapunov exponents **(D)**. The exponent values (small positive, zero and negative) indicate that the system displays low-dimensional chaotic dynamics. Adapted from [35].

dendrodendritic gap junction connectivity is crucial in the organization of such timing signal. Ensemble activity in the IO is organized dynamically using neuronal synchronization as a way of rapidly engaging or disengaging a given neuron within a synchronized group. This arrangement leads to generation of spatio-temporal patterns of activity into dynamic clusters that depend on the modulation generated by the connectivity of the system with external stimuli and with other levels with in the CNS. Indeed, such clustering results from interaction among IO neurons and external stimuli.

In our mathematical approach to model IO dynamics we started with nonlinear mathematical analysis of experimental data [49] from single neurons (Fig. 3) and from coupled pairs of IO neurons (Fig. 2). In this type of analysis it is essential to address the issue of noise and to clearly separate a noisy periodic oscillator form a non linear one. In the case of the IO our results indicate that the noise level is adequately low. In particular, the false nearest neighbors (FNN) and average mutual information (AMI) results clearly indicate that nonlinearity in the IO is not disguised noise.

Moreover the length of our experimental time series amply meet the condition for determining the Lyapunov exponents. Indeed, the results indicate that despite being almost perfectly periodic, IO oscillations have a weakly chaotic nature [35]. This property markedly increases the sensitivity of the dynamics, independently of input origin. Surprisingly, in this neuronal system the chaotic degree of the dynamics does not grow (that is the Lyapunov spectrum stays practically the same) regardless of the number of elements in the system. Indeed, the synchronization itself was found to belong to a very specific type known as chaotic phase synchronization, a notoriously robust dynamic system [35]. Chaotic synchronization has important advantages over the "normal" synchronization from being more "flexible" with respect to engaging and disengaging to probably providing "energy" gain as it requires smaller coupling strength.

If the IO were to play a role in movement coordination, it must be able to control functional parameters in time, in locality and in number of degrees of freedom. We have proposed [35] that to meet these requirements the IO uses its intrinsic oscillatory properties for temporal organization: its ability to organize, support and change clusters size and location to control spatial patterns of activity. In addition, its weakly chaotic properties exhibit the necessary fluidity to control the number of degrees of freedom by rapidly modulating the phase relation between clusters.

Our results from computer simulation of single neurons [36], and a network of considerable number of neurons [31] unequivocally support this view of IO functional dynamics.

Based on this phenomenological approach, we succeeded to reproduce the main dynamic features of the IO neuron and to

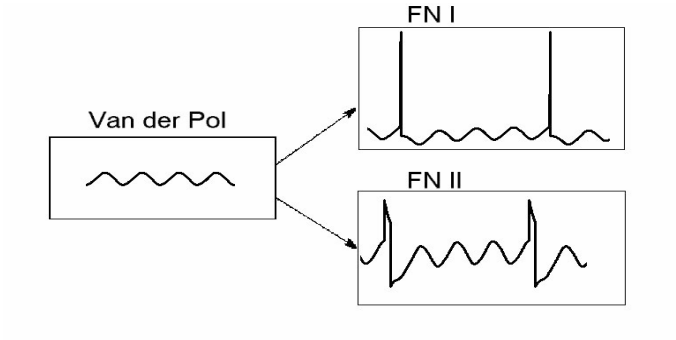

Fig 4. Demonstration of model properties. On the left, subthreshold oscillation. On the right, FNI and FNII demonstrate the two different levels of spike activation occurring at the apex of the oscillation. Adapted from [36].

implement variable electrotonic coupling amongst them. Furthermore, the simulated network of locally coupled neurons demonstrated clustering had similar features as those observed in *in vitro* IO slices with voltage-sensitive dyes. Our main conclusion from this study is that the IO is a truly integrated system where the neuronal network and the macroscopical dynamic features (cluster permutation agility) are so well matched that their control properties almost match cellular time constants. This allows the system effectively control uncountable number of movements without overloading brain function.

We introduced two mathematical models (see below), a single IO neuron model and an IO network model, to account for the IO function as a timing signal during motor control. These models were intended to serve as numerical prototypes for future hardware implementation and therefore were oriented to capture only those aspects of IO dynamics that critical for such initial implementation. The first model was developed to mimic membrane potential dynamics of IO neuron and in doing so to become the template for the development of a hardware microcircuit. The second model helped us to understand collective behavior – clustering, in IO. Further sophistication, as e.g. including such weakly chaotic subthreshold oscillations, in the existing hardware prototypes will improve performance.

Single Neuron Model

This model is based on electrophysiological properties observed in slice IO recordings [21], [35]. Their main features are: 1) autonomous subthreshold activity, weakly chaotic oscillations (by "weakly chaotic" we mean periodic and close to regular oscillatory dynamics with sufficient variability to support a positive value of the biggest Lyapunov exponent) [35]. 2) Subthreshold oscillation and the presence of two levels of spike initiation. 3) The system demonstrates subthreshold oscillatory phase preservation following spike generation. Based on these properties we considered a model (Fig. 4) that mimics an IO neuron dynamics as described above.

The model is composed of three autonomous interacting blocks responsible for the different functional modes observed experimentally [36]. The first block provides quasiharmonic oscillations. The other two blocks are responsible for spike generation at different thresholds.

As a particular implementation of the model we set:

$$
\begin{aligned}
x' &= y, && (1A)\\
y' &= (\gamma(1+\alpha u) - x^2)y - \omega^2(1+\beta u)x,\\
\varepsilon w' &= g(w) - z - x, && (1B)\\
z' &= 0.5(w - I_2)(w^2 + 0.1),\\
\varepsilon u' &= f(u) - v + hw, && (1C)\\
v' &= 0.05(u - I_1)(u^2 + 0.5),
\end{aligned}
\qquad (1)
$$

where the variable u accounts for the membrane potential of the neuron, the parameters γ and ω account for amplitude and frequency of quasiharmonic (subthreshold) oscillations. The coefficients α and β change the amplitude and frequency of oscillations depending on the membrane potential, u. The parameter h determines the strength of coupling between the two FitzHugh-Nagumo (FN) subsystems. $\varepsilon << 1$ defines the relaxation scale of the FN block. Note that while we made them identical they may have two different time scales here. For our purpose we fixed the parameters $\varepsilon = 0.01$, $\gamma = 0.21$, $\omega^2 = 0.63$, $a=1.8$, $b=0.5$, $h=0.5$ and took I_1, I_2 as control parameters playing the (qualitative) role of a constant current stimulus that changes the membrane potential level.

System (1) consists of three interacting subsystems. The first subsystem (1A) (variables (x,y)) represents a Van der Pol (VdP) oscillator providing robust quasiharmonic oscillations. The other two subsystem (1B) and (1C) ((u,v) and (w,z) variables) are based on FitzHugh-Nagumo (FN) mathematical model and are responsible for high- and low- threshold level spike generation respectively. The nonlinear functions $f(u)$, $g(w)$ are of cubic-shape form. For convenience, we approximate them in the piece-wise linear forms:

$$
f(u) = \begin{cases} -1.5\,u, & \text{if } u < a,\\ 0.2u - 1.7a, & \text{if } a < u < 4,\\ -1.6u - 1.7a + 9.6 & \text{if } u > 4. \end{cases}
$$

and (2)

$$
g(w) = \begin{cases} -2w, & \text{if } w < b,\\ 3w - 5b, & \text{if } b < w < 1,\\ -5w - 5b + 8 & \text{if } w > 1, \end{cases}
$$

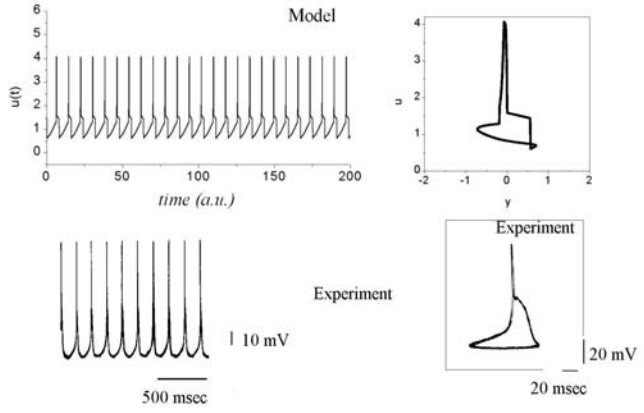

Fig. 5 Upper panels: Single IO neuron model showing oscillatory activity and Lissajeu plot for the model. Lower panels: Results obtained from single intracellular cell recording from the IO cells . Adapted from [36].

where the parameters "*a*" and "*b*" define the high- and low-threshold values, respectively. The values of the coefficients in (2) characterize width, height and refractory period of the pulses (spikes) generated from the two thresholds.
The model proved to be fully consistent with experimental data, capable of reproducing all main features of IO neuron membrane potential dynamics (Fig. 4).

Network model

The motivation behind modeling neuronal activity clusters was that of testing the assumption that such clustering and cluster size are electrotonic-coupling dependent. Indeed, while this assumption may be considered obvious at first glance, it has been demonstrated that activity profiles other than clusters (such as spirals, waves, concentric rings) can occur in coupled neuronal networks [45].

The experimental data provided parameters such as: membrane potential oscillation (from intracellular recordings) and cluster size and shape and their modulation by pharmacological intervention (from voltage-sensitive dye imaging [31]). These parameters define the model type. The network properties were modeled by interconnecting a set of model neurons into a two dimensional matrix with isotropic coupling properties. Such model was easier to implemented and scaled than models that incorporate single cell cable and ionic conductance properties [26], [46].

Single neurons are represented as distinct elements (points) in a rectangular four point connectivity lattice. Each element is endowed with quasi-periodic oscillatory properties defined by a set of equations having a periodic and a noise term as follows:

$$z' = z\,(i\,w_0 - \gamma) + i\,\sqrt{2D}\,\xi\,(t) \qquad (3)$$

where the variable z characterizes neuron dynamics (with $x = Re\,(z)$ i.e. $z = x + iy$, prime implies differentiation), i is an imaginary unit, x and y are real numbers), γ is a damping constant, w_0 is angular oscillation frequency in the absence of noise and damping ($w_0 = 2\pi * 10$ Hz), D is a parameter determining noise intensity scaling and $\xi(t)$ is a noise term which has zero mean with a time correlation function given by

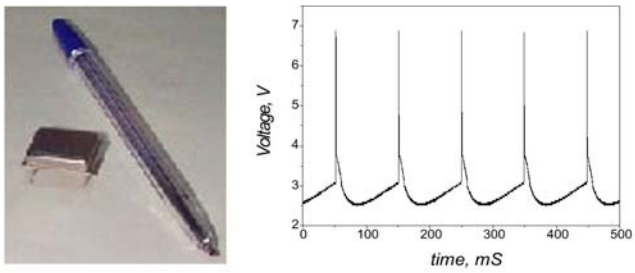

Fig. 6 Left panel: Electronic microchip implementing the UCS control unit. Right panel: Unit oscillation with maximum spike frequency. Adapted from [48].

$$\langle \xi_{jk}(t)\,\xi_{lm}(t')\rangle = \delta_{jk}\,\delta_{lm}\,\delta(t-t') \qquad (4)$$

where the brackets imply average, and δ denotes a function which is zero when its argument has a non-zero value. Relatively regular oscillations have variable amplitude with sharp frequency peak in the region of 10 Hz, which is in good agreement with *in vivo* experimental data [47].

IV. Computer Model Hardware Implementation: The Universal Control System (UCS)

With the above in mind, and given the space-time dynamics of the oscillatory olivo-cerebellar system, we decided to implement the cluster control principles of the olivo-cerebellar system. These clusters, as described in the imaging part, consists of sets of IO neurons that oscillate in phase. This was implemented using a set of hard wired hybrid electronic chips (Fig. 6) each representing an IO neuron organized in a circuit which resembles some of the network properties of the olivo-cerebellar system. We refer to this harware device as a Universal Control System (UCS) given the fact that the olivo-cerebellar system is presented in all vertebrate forms.

The UCS "computing" power had been expected to be substantially higher than that implementable with a digital computer. We found using a computer simulation to model the UCS [48] that given N parameters to be controlled the UCS would need to operate optimally at least the same number of oscillatory units. The results indicated that a unit oscillator may hold the specific phase that controls the state of a given parameter [48]. Thus, let M be the number of levels of phase that could be resolved by the system, then, at the timing interval τ the UCS would "compute "M^N possible combinations of different parameter states. In terms of digital processing the upper limit of the UCS computing power

would be:

$$P(\tau) \sim \frac{M^N}{\tau} \quad \textbf{(5)}$$

In the olivo-cerebellar system the precision of spike synchrony and hence the time resolution is high. Experiments showed that spikes associated with the same oscillatory cluster are generated in a ≈ 1ms time window [48]. Thus, the number of possible states for a 100 ms period can be estimated as M=100. Note that in the UCS the timing window can be substantially decreased down to the energetic limits of the constituent materials. Formula 5 gives only the upper limit for the UCS. Within any particular template of activity the number of possible states will be smaller and will depend on the particular task the template is required to accomplish. Compared to a digital system this resembles the limits which a particular operating system or algorithm imposes on the speed of calculations.

V. Conclusions and Implications

On the basis of the anatomy of the IO nucleus and the widespread complex synchronicity across the cerebellar mantle, it has been proposed that functionally the IO is organized in clusters of synchronously oscillating neurons that can generate rhythmic and coherent activity in the cerebellum [43]. In agreement with this proposal, we were able to visualize the IO oscillatory clusters and described their spatio-temporal profiles *in vitro*.

Our optical imaging responses from the IO nucleus consisted of initial antidromic activation of the area around the stimulating electrode that was followed by the stimulus reset ensemble IO oscillations. The optically recorded IO oscillations emanated from several spatially separated fluorescent clusters that had the same oscillation frequency and were phase coherent. Our experiments with picrotoxin indicate that borders of these clusters were most likely determined by the level of effective electrotonic coupling among the IO cells and therefore by the state of the IO network.

Implication of modeling results

Our modeling results support the conclusion that regulation of electrotonic coupling in the IO by feedback inhibition from the cerebellar nuclei regulates IO cluster coupling which control their distribution and size [11], [15], [31]. That is, increased inhibition results in cluster size reduction and in an increase in the number of independent clusters (Fig. 2F). Conversely, decrease of inhibition results in increased cluster size and a simultaneous decrease in the number of independent clusters (Fig. 2E). These modeling results are in agreement with our imaging data. The modeling results also support our two main working hypotheses. First, that the level of inhibition (i.e. coupling) is a main factor in regulating the average size of a cluster of synchronous activity. Second, that with the higher level of inhibition the number of clusters increases. For statistical analysis we used Markov Random Fields method described elsewhere [27], which allows quantitative estimation of the level of spatial organization. Interestingly cluster distribution is surprisingly stable and, counter intuitively, fluctuations in cluster organization are inhibition dependent: the higher level of inhibition the lower level of fluctuations. This is so both experimentally and as a modeling result. Furthermore high level of inhibition leads to a larger number of smaller clusters and thus into increased number of possible functional states and degrees of freedom.

Indeed, as the degrees of freedom increase with increased number of clusters, the probability of large fluctuations in cluster size decreases. In fact, the system becomes "less liquid" with larger number of smaller clusters. That is, despite the large number of clusters the system robustly preserves a particular level of spatial organization. More fundamentally, the results indicate the existence of a maximum number of possible functional states, implying that increased inhibitory feedback does not result in an ever-increasing control ability. That is, even at high levels of clustering the IO network demonstrates short phase resetting time (~ 70 ms) without loosing oscillatory robustness, thereby optimizing reset agility without sacrificing control [35].

Functional significance of the IO oscillatory clusters

Previous *in vivo* multielectrode experiments have shown that synchronized CSs are primarily observed among PCs located within the same parasagittal bands [9], [10], [16], [17]. Groups of IO neurons that define such parasagittal bands consist of up to several hundred of neurons [17]. Since this number is in the same order of magnitude as the calculated number of cells in our fluorescent clusters, we propose that our optical measurements might reflect the ensemble physiological properties formerly observed with multiple recordings at the PC level [31]. Hence, each IO cluster can control activity of a single parasagittal band in the cerebellum. Simultaneous activation of several IO clusters would result in coherent complex spike activity between different parasagittal bands as has been observed during coordinated movements.

Ultimately, as further insight is gained on the oscillatory property of neurons and their relation to macroscopic motor execution and control, a general message becomes apparent: The dynamic properties of single neurons and the channel kinetics that generate them seem to hone the "impedance matching" from the molecular to the macroscopic to the point that, as in the IO, our motor timing is no other than the echo of our IO oscillation.

References

[1] S. Ramon y Cajal, "Sobre las fibras nerviosas de la capa molecular del cerebelo", *Rev. Trimestr. Histol*, vol 2, pp. 33-41, pp. 1888.

[2] J. Szentagothai and K. Rajkovits, "Ueber den Ursprung der Kletterfasern des kleinhirns" *Z. Anat. Entwicklungsgeschichte*, vol. 121, pp. 130-41, 1959.
[3] J. C. Eccles, R. Llinás and K. Sasaki, "The excitatory synaptic action of climbing fibres on the purinje cells of the cerebellum", *J Physiol (Lond)*, vol. 182, pp. 268-96, 1966.
[4] W. T. Thach, "Discharge of Purkinje and cerebellar nuclear neurons during rapidly alternating arm movements in the monkey", *J Neurophysiol*, vol. 31, pp. 785-97, 1968.
[5] D. M. Armstrong and R. F. Schild, "A quantitative study of the Purkinje cells in the cerebellum of the albino rat" *J Comp Neurol*, Vol. 139, pp. 449-56, 1970.
[6] T. Eller and V. Chan-Palay, "Afferents to the cerebellar lateral nucleus. Evidence from retrograde transport of horseradish peroxidase after pressure injections through micropipettes", *J Comp Neurol*, vol. 166, pp. 285-301, 1976.
[7] W. E. Crill, "Unitary multiple-spiked responses in cat inferior olive nucleus", *J Neurophysiol*, vol. 33, pp. 199-209, 1970.
[8] R. Llinás and Y. Yarom, "Electrophysiology of mammalian inferior olivary neurones in vitro. Different types of voltage-dependent ionic conductances", *J Physiol (Lond)*, vol. 315, pp. 549-67, 1981
[9] C. C. Bell and T. Kawasaki, "Relations among climbing fiber responses of nearby Purkinje Cells", *J Neurophysiol*, vol. 35, pp. 155-69, 1972.
[10] R. Llinás and K. Sasaki, "The functional organization of the olivo-cerebellar system as examined by multiple PurKinje cell recordings", *Eur J Neurosci*, vol. 1, pp. 587-602, 1989.
[11] E. J. Lang, I. Sugihara and R. Llinás, "GABAergic modulation of complex spike activity by the cerebellar nucleoolivary pathway in rat", *J Neurophysiol*, vol. 76, pp. 255-75, 1996.
[12] M. Fukuda, T. Yamamoto and R. Llinás, "The isochronic band hypothesis and climbing fiber regulation of motricity: an experimental study", *Eur J Neurosci*, vol. 13, pp. 315-26, 2001.
[13] R. Llinás, R. Baker and C. Sotelo, "Electrotonic coupling between neurons in cat inferior olive", *J Neurophysiol*, vol. 37, pp. 560-71, 1974.
[14] C. Sotelo, R. Llinás and R. Baker, "Structural study of inferior olivary nucleus of the cat: morphological correlates of electrotonic coupling", *J Neurophysiol*, vol. 37, pp. 541-59, 1974.
[15] R. Llinás 1974. Eighteenth Bowditch Lecture. Motor aspects of cerebellar control. Physiologist, vol. **17**: 19-46.
[16] E. J. Lang, *et al.*, "Patterns of spontaneous purkinje cell complex spike activity in the awake rat", *J Neurosci*, vol. **19**, pp. 2728-39, 1999.
[17] T. Yamamoto, M. Fukuda and R. Llinás, "Bilaterally synchronous complex spike Purkinje cell activity in the mammalian cerebellum", *Eur J Neurosci*, vol. 13, pp. 327-339, 2001.
[18] R. Llinás and M. Muhlethaler, "Electrophysiology of guinea-pig cerebellar nuclear cells in the in vitro brain stem-cerebellar preparation", *J Physiol (Lond)*, vol. 404, pp. 241-58, 1988.
[19] J. P. Welsh, E. J. Lang and R. Llinás, "Dynamic organization of motor control within the olivocerebellar system", *Nature*, vol. 374, pp. 453-7, 1995
[20] R. Llinás and Y. Yarom, "Properties and distribution of ionic conductances generating electroresponsiveness of mammalian inferior olivary neurones in vitro", *J Physiol (Lond)*, vol. 315, pp. 569-84, 1981.
[21] R. Llinás and Y. Yarom, "Oscillatory properties of guinea-pig inferior olivary neurones and their pharmacological modulation: an in vitro study", *J Physiol (Lond)*, vol. 376, pp. 163-82, 1986.
[22] L. S. Benardo and R. E. Foster, "Oscillatory behavior in inferior olive neurons: mechanism, modulation, cell aggregates", *Brain Res Bull*, vol. 17, pp. 773-84, 1986.
[23] T. Bal and D. A. McCormick, "Synchronized oscillations in the inferior olive are controlled by the hyperpolarization-activated cation current I(h)", *J Neurophysiol*, vol. **77**, pp. 3145-56, 1997.
[24] I. Lampl and Y. Yarom, "Subthreshold oscillations and resonant behavior: two manifestations of the same mechanism", *Neuroscience*, vol. 78, pp. 325-41, 1997.
[25] B. Hutcheon and Y. Yarom, "Resonance, oscillation and the intrinsic frequency preferences of neurons", *Trends Neurosci*, vol.23, pp. 216-22. 2000.
[26] Y. Manor, J. Rinzel, I. Segev and Y. Yarom "Low-amplitude oscillations in the inferior olive: a model based on electrical coupling of neurons with heterogeneous channel densities", *J Neurophysiol*, vol. **77**, pp. 2736-52, 1997.
[27] V. Makarenko, E. J. Lang and R. Llinás, "A new approach to the analysis of multidimenshional neuronal activity: Markov Random Fields", *Neural Networks*, vol. 10, pp. 785-789, 1997.
[28] M. V. Bennett, "Electrical synapses, a personal perspective (or history)", *Brain Res Brain Res Rev*. vol. 32, pp.16-28, 2000.
[29] C. I. De Zeeuw*, et al.*, "Morphological correlates of bilateral synchrony in the rat cerebellar cortex", *J Neurosci*, vol. 16, pp. 3412-26, 1996.
[30] B. J. Fredette and E. Mugnaini, "The GABAergic cerebello-olivary projection in the rat", *Anat Embryol*, vol. 184, pp. 225-43, 1991.
[31] E. Leznik, V. Makarenko and R. Llinás, "Electrotonically mediated oscillatory patterns in neuronal ensembles: an in vitro voltage-dependent dye-imaging study in the inferior olive", *J Neurosci*, vol. 22, pp. 2804-15, 2002.
[32] E. J. Lang, "Organization of olivocerebellar activity in the absence of excitatory glutamatergic input", *J Neurosci*, vol. **21**, pp. 1663-75, 2001.
[33] E. J. Lang, "GABAergic and glutamatergic modulation of spontaneous and motor-cortex- evoked complex spike activity", *J Neurophysiol*, vol. 87, pp. 1993-2008. 2002.
[34] T. J. Ebner and G. Chen, "Use of voltage-sensitive dyes and optical recordings in the central nervous system", *Prog Neurobiol*, vol. 46**,** pp. 463-506, 1995.
[35] V. Makarenko and R. Llinás, "Experimentally determined chaotic phase synchronization in a neuronal system", *Proc Natl Acad Sci U S A*, vol. 95, pp. 15747-52, 1998.
[36] M. G.Velarde*,* V. Kazantsev, V. Makarenko, V. Nekorkin and R. Llinás, "Modeling inferior olive neuron dynamics", *Neural Networks*, vol.15**,** pp. 5-10, 2002.
[37] A. F. Bleasel, and A. G. Pettigrew, "Development and properties of spontaneous oscillations of the membrane potential in inferior olivary neurons in the rat" *Brain Res Dev Brain Res.*,vol. 65: 43-50, 1992.
[38] C. T. Sotelo, T. Gotow and M. Wassef, "Localization of glutamic-acid-decarboxylase-immunoreactive axon terminals in the inferior olive of the rat, with special emphasis on anatomical relations between GABAergic synapses and dendrodendritic gap junctions", *J Comp Neurol.*, vol. 252,pp. 32-50, 1986.
[39] C. I. De Zeeuw, I. Holstege, J. C.Ruigrok, and J.Voogd, "Mesodiencephalic and cerebellar terminals terminate upon the same dendritic spines in the glomeruli of the cat and rat inferior olive: an ultrastructural study using a combination of [3H]leucine and wheat germ agglutinin coupled horseradish peroxidase anterograde tracing", *Neuroscienc,*vol. 34, pp. 645-55, 1990.
[40] A. Grinvald, E. E. Lieke, R. D. Frostig and R. Hildesheim, "Cortical point-spread function and long-range lateral interactions revealed by real-time optical imaging of macaque monkey primary visual cortex", *J Neurosci*., vol. 14, pp, 2545-68, 1994.
[41] J. J. Cunningham, R. M. Sherrard, K. S. Bedi, G. M. Renshaw and A. J. Bower, "Changes in the numbers of neurons and astrocytes during the postnatal development of the rat inferior olive", *J Comp Neurol*., vol. 406, pp. 375-83, 1999.
[42] C. I. De Zeeuw, J. I. Simpson, C. C. Hoogenraad, N. Galjart, S. K. Koekkoek, T. J. Ruigrok, "Microcircuitry and function of the inferior olive", *Trends Neurosci*., vol. 21, pp. 391-400, 1998.
[43] J. P. Welsh and R. Llinás, "Some organizing principles for the control of movement based on olivocerebellar physiology", *Prog Brain Res.*, vol. 114, pp. 449-61, 1997.
[44] T. J. Ruigrok and J. Voogd, "Cerebellar influence on olivary excitability in the cat", *Eur J Neurosci*., vol. **7,**pp. 679-93, 1995.
[45] V. I. Makarenko, "Neural network with embedded oscillators", *Biological Bulletin*., vol. 187, pp. 256-257, 1994.
[46] N. Schweighofer, K. Doya and M. Kawato, "Electrophysiological properties of inferior olive neurons: A compartmental model", *J Neurophysiol*., vol. 82, pp. 804-17, 1999.
[47] K. Sasaki, J. M. Bower and R. Llinás, "Multiple Purkinje cell recording in rodent cerebellar cortex", *Eur J Neurosci*., vol. 1, pp. 572-586, 1989.
[48] V. B. Kazantsev, V. I. Nekorkin, V. I. Makarenko and R. Llinás, "Olivo-cerebellar cluster based universal control system", Submitted for publication, *PNAS USA*, 2003.
[49] H. Aberbanel, Analysis of observed chaotic data. New York: Springer, 1995.